Multiparticle random walks on a deformable medium

Sheng-You Huang, Xian-Wu Zou,* and Zhun-Zhi Jin
Department of Physics, Wuhan University, Wuhan 430072, People's Republic of China
(Received 13 May 2002; published 24 October 2002)

Multiparticle random walks on a deformable medium have been investigated in $(2+1)$ dimensions. The time evolution of the particle distribution is studied. The results show that the randomly distributed particles in the beginning will be self-organized into a cluster pattern in the intermediate stage, and then return to the random distribution pattern in the late stage. The dependence of the clustering degree on the stiffness parameter of medium α, stability parameter of systems β, and average particle density ρ_0 is also investigated. There exists an optimal clustering stability β_p, at which the system has the strongest clustering ability and corresponds to a maximum clustering coefficient Γ_p^*. The dependence of the optimal clustering coefficient Γ_p^* on the stiffness α and particle density ρ_0 is obtained, and the landscape of the medium generated by particles is also investigated.

DOI: 10.1103/PhysRevE.66.041112 PACS number(s): 05.40.Fb, 05.10.Ln, 89.75.Fb

I. INTRODUCTION

Because of the interest in both physics and mathematics communities, random walks (RW) and its applications have been extensively investigated in variety of fields [1–7]. The behavior of a large class of natural and social systems in science (physics, chemistry, ecology, and economy) can be cast into the form of random walks [1,2]. In previous years, based on purely random walks (i.e., Brownian motion) various models of random walks with memory or interaction have been studied in order to account for distinct features of physical, chemical, and biological systems, whose complexity goes beyond what can be obtained from the simple random walk picture [8–16]. The self-avoiding walk is the first RW model considering partially the influence of the environment. In this model, the walker is prohibited to visit the sites visited before in order to account for the repulsion between two molecules that are close together. The model has been found useful for investigating polymers in dilute solution [8]. Considering the truly growing phenomena, Amit *et al.* have introduced a model called true self-avoiding walks [9]. In the model the walker jumps at each step to one of the neighboring sites with a probability depending on the number of times the new site has been visited in the past. The Domb-Joyce model is a model based on the weighting of turning points, whose behavior is related to that of an Ising spin chain [10]. Stanley *et al.* have proposed a model of interacting random walks in which each new site visited has a weight factor [11]. The model displays some of the intriguing features of diffusion on random fractals, and also describes polymer chains with either repulsion or attraction. The self-attracting walk is also investigated in which the probability for a walker jumping to a given site is exp $(-nu)$ with $u<0$, where $n=1$ for the sites visited by the particle at least once and $n=0$ for the others [12]. This model shows a critical crossover with the attractive parameter increasing [13,14]. The ''true'' self-attracting walk is an extended version of the self-attracting walk, and in this walk the jumping probability is related to the number of times visited a site is. The model also shows the similar crossover behavior [15]. Lam and co-worker have proposed the active random walk model [16]. In that model, the walker moves in a potential (landscape). The potential is changed by the walker according to the landscape function. Lam and co-worker proposed two types of landscape functions for use [16]. The random walks with the memory enhancement and decay have also been studied in two dimensions [17]. It shows that there exist two different classes of walks. The random walks with a nonzero decay exponent belong to the same class as purely random walks, while the random walks for the nondecaying case fall into the true self-attracting walk class.

In a very recent paper by our group [18], a model of random walks on a deformable medium has been proposed. Different from the simple interacting random walks such as the self-avoiding walks, self-attracting walks, etc. [8,10–12], our model counts in the cumulative memory effects of the walk by deforming the medium at each step [18]. Although the generalized interacting random walk models also take into account the memory effects [9,13–17], the introduction of a memory parameter in these models is somewhat unnatural. In our model, the walker moves on a true medium and thereby has a clear physical picture [18]. The model presents a useful method for investigating the random walks in the case when interactions exist between the walker and its environment. Namely, considering the whole of environment as a field or potential, in the walk the walker changes the field (potential) of environment at the visited site and in turn the variation of the field (potential) affects the motion of the walker afterwards. This is a common phenomenon for many complex systems in natural and social sciences, such as river formation, food seeking of ants, movement of the heat-seeking missile, and so on [16–22]. The model exhibits rich behaviors, including a ''localization-delocalization'' phase transition as the stiffness and stability parameters are varied [18].

In the random walk models mentioned above, attention is mostly focused on the characteristics associated with the

*Author to whom correspondence should be addressed. Email address: xwzou@whu.edu.cn

wandering of a single walker [2]. In fact, almost all the systems consist of many individuals or elements in nature or society. However, the behaviors of a set of random walkers are much less known, notwithstanding their interest [23–25]. In a multiparticle system the random walkers present many special phenomena because of the interactions between the walkers and environments as well as those between the walkers. One of the most interesting characteristics is the collective motion of particles, which may be related to the migration of locusts, flocks of flying birds, animal grouping habit, collective behavior of robots, and so on. Vicsek *et al.* have introduced a simple model of self-propelled particles in order to investigate the emergence of self-ordered motion in systems of particles with biologically motivated interaction [26], in which particles are driven with a constant absolute velocity and at each time step assume the average direction of motion of the particles in their neighborhood with some random perturbation added. The model exhibits a type of kinetic phase transition from no transport to finite net transport. Considering the physical properties of active elements with mutual interactions, Shimoyama *et al.* proposed a mathematical model of collective motion [27]. The model exhibits several kinds of cluster motion seen in nature, including collective rotation, chaos, and wandering. Bussemaker *et al.* also presented a cellular automation model for random walkers with biologically motivated interactions favoring local alignment [28]. The model leads to collective motion or swarming behavior, and a dynamical phase transition exhibiting spontaneous breaking of rotational symmetry occurs at a critical parameter value. Considering a finite-size flock, Levine *et al.* presented a discrete model consisting of self-propelled interacting particles that obey simple rules [29]. The self-organization in the model can lead to a localized flock of finite extent. These dynamical models can give pictures of the cooperative motion for multiparticle systems, but the interactions between particles are somewhat unnatural.

In the above multiparticle models, the collective motion results from the direct interaction between particles [25–29]. Very recently, the patterns of particle distribution were investigated in multiparticle systems by the random walks with memory enhancement and decay [30]. Although there exists no direct interaction between particles, the model also exhibits a similar collective behavior. In this paper, we investigate the multiparticle random walks on a $(2+1)$-dimensional deformable medium. In the model, the nondirect interacting particles move in a true potential. Of interest is that the present model exhibits a cluster state for the particle distribution. The time evolution of the particle distribution and its dependence on the average particle density, stiffness of medium as well as the stability of systems are studied by extensively numerical simulations and also a simple theoretical analysis. The present work will be helpful to understand the motion behaviors of particles in complex multiparticle systems with interactions between elements and their environment. These behaviors appear to be the specific property of the collective motion for multiparticle systems, which is distinct from the motion of a random walker interacting with the environment.

II. MODEL AND METHOD

The model used here is the same as that in the previous paper [18]. To characterize the interactions between the particles and medium, the most important work is establishing the expressions of the deformation of the medium made by the walker in the medium. In the present work, the deformation of the medium is depicted by the Kelvin-Voigt model [31]. The model can describe the deformation modes of many materials in nature under a load, such as soil, rubber, and so on. According to the Kelvin-Voigt model [31], under a constant stress σ_0 the variation of the deformation of medium ε with time t can be expressed by an exponential form

$$\varepsilon(t)=\varepsilon_\infty(1-e^{-\alpha t}), \tag{1}$$

where ε_∞ is the maximum deformation at the time $t\to\infty$, and α is a parameter concerned with the properties of the medium compressed. The parameter α is named as the stiffness parameter of the medium. The larger the parameter α is, the harder the further deformation of the medium is.

In the walk, the retention period of the walker per visit is expressed by τ. The force σ_0 applied on the deformable medium is the weight G of the walker. Without loss of generality, we take ε_∞, G, and τ as the length, force, and time units, respectively. Thus, the deformation magnitude at site (i,j) after n visits can be described as

$$\varepsilon_n(i,j)=1-e^{-\alpha n(i,j)}, \tag{2}$$

where $\varepsilon_n(i,j)$ can be regarded as the landscape or potential of the deformable medium at site (i,j). Therefore, the probability with which the walker moves from site (i,j) to a nearest neighbor (i',j') depends on the difference between the deformation at site (i,j) and that at site (i',j'). It can be expressed by

$$P\{(i,j)|(i',j')\}\propto\exp\{-\beta[\varepsilon_n(i,j)-\varepsilon_{n'+1}(i',j')]\}, \tag{3}$$

where $\beta=1/k_BT$, k_B is the Boltzmann constant and T is the ''temperature'' of systems. Since the randomness of the walk reduces with the increase of β, for convenience the parameter β is called as the stability of the system.

The deformable medium is represented by using a two-dimensional (2D) square lattice of size $L\times L$ with periodic boundary conditions. Monte Carlo (MC) simulations have been used to study the movement of N random walkers on the deformable medium. Initially the surface of the medium is flat with the deformation magnitude being zero at each site, and the particles are randomly distributed in the lattice with the average particle density $\rho_0=N/L^2$. At each MC step, a particle is selected at random and makes an attempt to move to a chosen nearest-neighbor site according to the probability of Eq. (3). If the chosen site has been occupied by the other particle, the movement is not accepted; otherwise, the movement is performed. Then, the visiting time n at the site occupied by the attempted particle is enhanced by one and the walk comes into the next MC step. After each MC step the ''time'' is increased by $1/N$, such that after 1 time step, on the average, all particles in the system have

attempted to jump. It should be noted that the present ''time'' is not the true time, and we call it as the ''quasitime.'' When the present model is applied to the biological systems, the present ''time'' may correspond to the true time. For the pure physical systems, the present definition of time is not consistent with that of the true time, because the jump probability of the walker is different at different time steps, which results in different jump time. In the pure physical systems, the definition of true time can be obtained by choosing one walker and jump direction with a global normalized probability. However, the definition of time is not much relevant in the present model because we focus on the pattern evolution of the particle distribution. Therefore, for simplicity, we use the above definition of quasitime to save the computation time. It will be shown in the following section that there exists only a slight difference between the results from these two types of definition of time.

We regard a group of particles as a cluster in which the particles adjoin one after another. The definition of a cluster is described as any two particles that are nearest neighbors and belong to the same cluster [32]. To characterize quantitatively the clustering phenomenon of the particle distribution in the multiparticle systems, we introduce the average cluster size $S(t)$ of the systems, which is the weight average of the number of particles per cluster and is expressed as [32,33]

$$S(t)=\frac{\sum_s s^2 n_s(t)}{\sum_s s n_s(t)}, \tag{4}$$

where $n_s(t)$ is the number of clusters with s particles at the time t. Thus, the clustering degree of systems can be described by the size-independent clustering coefficient

$$\Gamma(t)\equiv\frac{S(t)-1}{N-1}, \tag{5}$$

where N is the number of particles in the system. It can be seen that the value of Γ changes from 0 to 1.0. The larger the coefficient Γ is, the higher the clustering degree of the system is. When $\Gamma=0$, the particles do not cluster and are separated from each other; when $\Gamma=1.0$, the system has the maximum clustering degree and all particles in the system are connected to one cluster.

III. RESULTS AND DISCUSSION

We have investigated the time evolution of the pattern of the particle distribution and its dependence on parameters α, β, and ρ_0 in 2D multiparticle systems. For comparison, the number of particles is chosen to be about $N=1000$ for different systems. Namely, the lattice size is taken as $L=\mathrm{int}[(1000/\rho_0)^{1/2}]$, where int$[x]$ denotes the largest integer X such that $X<x$. The stiffness parameter α takes value in the interval $[0.001,0.1]$. To remove the fluctuation, all the results are taken from the averaging over at least ten independent realizations.

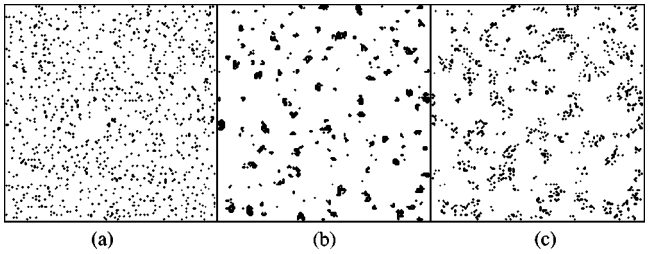

FIG. 1. The evolution of the particle distribution pattern for the multiparticle system with the parameters $\alpha=0.005$, $\beta=5.62$, and $\rho_0=0.05$; time $t=20$ (a), 1500 (b), and 100 000(c).

Figure 1 shows the pattern evolution of the particle distribution for the multiparticle system with the stiffness $\alpha=0.005$, stability $\beta=5.62$, and particle density $\rho_0=0.05$. It can be seen from Fig. 1 that with the passage of time going the pattern of the particle distribution varies. The distribution exhibits a random dispersive pattern in the early stage, then appear clusters which disperse in the whole lattice in the intermediate stage, and returns to the random dispersive pattern in the late stage. To quantify the distribution of particles, we calculate the clustering coefficient $\Gamma(t)$ of the system. Figure 2 shows the evolution of the clustering coefficient $\Gamma(t)$ with time t for several systems with the same parameters $\alpha=0.005$ and $\rho_0=0.05$ but different β values. It can be seen from Fig. 2 that there exists a maximum value Γ^* at an intermediate time t^* for each β, and Γ^* varies with β. For comparison, Fig. 2 also shows some corresponding results obtained from the definition of true time in which the particles jump with a global normalized probability. As we can see from Fig. 2, the difference between the results from two types of definitions of time is very small. This indicates that the simulation results are reasonable by using the present definition of quasitime.

The behaviors in Figs. 1 and 2 can be explained as follows. In the initial stage of the walk, the deformation of medium is very small and the surface of the medium is al-

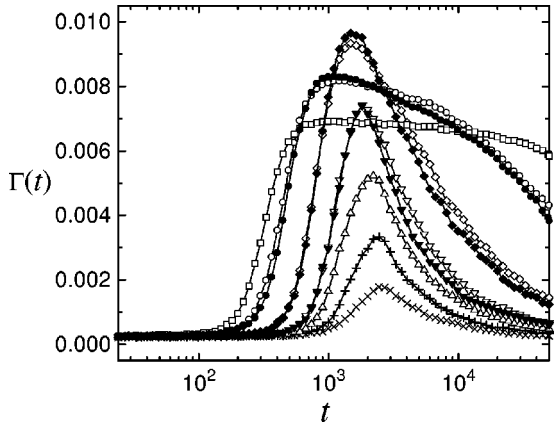

FIG. 2. The evolution of the clustering coefficient $\Gamma(t)$ with time t at parameters $\alpha=0.005$ and $\rho_0=0.05$ for the stability $\beta=3.16$ ($\times$), 3.55 ($+$), 3.98 ($\triangle$), 4.47 (∇), 5.62 ($\diamond$), 7.94 ($\bigcirc$), 10.0 ($\square$). For comparison, we also plot some corresponding results from the definition of true time (solid symbols), in which the particles jump with a global normalized probability.

most flat, so the particles move randomly in the lattice as with initiation. Moreover, in this stage the drift distance of a particle does not attain the average distance between neighboring particles, the particles have few chances to meet, and most of particles are separated from each other. Thus, the distribution of particles remains the random dispersive pattern [see Fig. 1(a)] and the clustering coefficient Γ has a very small value [see the short-time end of Fig. 2]. After a long time, each site in the lattice has been visited many times by particles and the deformation at those sites has reached a large value close to the maximum deformation [18]. Namely, the deformed medium can be considered as a smooth plane in this stage. In this case, the particles make purely random walks in the medium and the distribution of particles also shows a random dispersive pattern with a small value of Γ [see Fig. 1(c) and the long-time tails of Fig. 2].

However, in the intermediate stage of the walk, the particles have performed walks with a certain number of steps and the trajectories generated by neighboring particles overlap partly. The walking of particles deforms the medium. The deformed medium can be described by the complex landscape with valleys and apexes [18]. In this situation, the particles will tend to gather in the valleys and form groups. The motions of the particles in the same group are influenced by sharing the deformation region generated mainly by the particles in this group. Because the particles prefer to walk toward the sites with the larger deformation, the particles in the same group concentrate gradually and form a cluster after certain time steps. Therefore, the distribution of particles appears a clustering phenomenon [see Fig. 1(b)] and there exists a maximum value Γ^* of the clustering coefficient in each Γ-t curve of the system (see Fig. 2). For convenience, we call the maximum value Γ^* as the characteristic clustering coefficient, which characterizes the clustering degree of particles in a system.

Figure 2 also shows that increasing the stability parameter β widens the Γ-t curves. This mainly results from the fact that the larger β leads to a stronger localization of particles, and thereby the diffusion of particles is slower [18].

From Fig. 2 we can also find that for a fixed stiffness α there exists an optimal clustering stability β_p at which the system has the strongest clustering ability. As β is less or larger than β_p, the characteristic clustering coefficient Γ^* reduces. At the optimal clustering stability $\beta_p \approx 5.62$, there exists an optimal clustering coefficient $\Gamma_p^* \approx 0.0093$ (see the curve symbolized by diamonds in Fig. 2). In Fig. 3 we plot the characteristic clustering coefficient Γ^* as a function of the stability β at the particle density $\rho_0 = 0.05$ for several different α values. It can be seen from Fig. 3 that as the stability β increases, the characteristic clustering coefficient Γ^* first increases to a maximum value Γ_p^*, and then reduces. From Fig. 3 we can also see that the optimal clustering stability β_p is almost independent of the stiffness α, but the optimal clustering coefficient Γ_p^* increases drastically with the reduction of α.

The dependence of the characteristic clustering coefficient Γ^* on the stability β in Fig. 3 can be explained as follows. When the stability parameter β is very small ($\ll \beta_p$), the

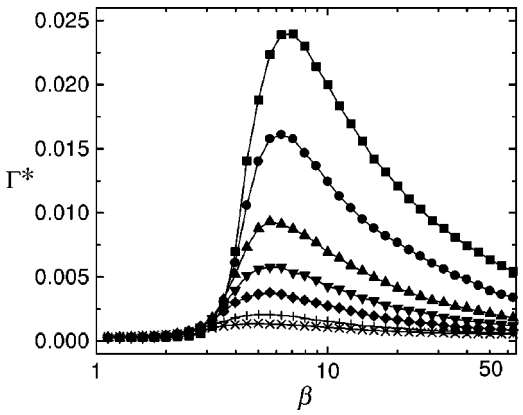

FIG. 3. The characteristic clustering coefficient Γ^* as a function of the stability β at the particle density $\rho_0 = 0.05$. From top to bottom, stiffness $\alpha = 0.001,\ 0.002,\ 0.005,\ 0.01,\ 0.02,\ 0.05,\ 0.1$.

fluctuation of the system is very strong. The motions of particles are governed by the randomness of the system, and the particles perform approximately purely random walks irespective of the deformation [18]. In this case, the particles cannot join and are randomly distributed in the lattice. Therefore, the characteristic clustering coefficient Γ^* takes a very small value, which corresponds to that of randomly distributed particles (see Fig. 3). When the stability β is very large ($\gg \beta_p$), the randomness of the system is very weak and the motions of particles are determined by the deformation of the medium [18]. In this situation the trajectories of the particles are compact, surrounding their original sites. The particles are localized in their compact trajectories and diffuse in them. In this case, the medium at visited sites has almost reached the maximum deformation except the sites near the boundary of trajectories [18]. Thus, one can expect the particles to move independently before their meeting. After that, all the visited sites, which have almost reached the maximum deformation, are connected together. The particles will make purely random walks in the connected region with the maximum deformation and have a very small probability of jumping into the unvisited sites [18]. Therefore, in this situation the clustering degree of particles is expected to be not high, and the system also has a small value of Γ^* (see Fig. 3).

In the intermediate range of β, the effect of the deformation ε is comparable to that of the thermal fluctuation $1/\beta$ on the motions of particles [18]. On the one hand, because of the finite β value, the particles can easily move in the medium comparing with the case of large β, and have many chances to meet. On the other hand, the generated deformation may somewhat localize the motions of particles because the value of β is not very small [18]. In this case, once two particles meet they will share the deformation generated by each other and tend to group and form a cluster. The more the number of particles in a cluster is, the more advantageous the share of deformation is, and the more stable this cluster is. Correspondingly, one can expect that there exists an optimal clustering stability β_p at which the system is most favorable for the clustering of particles, and the characteristic clustering coefficient Γ^* has a maximum value Γ_p^* (see Fig. 3). In the following, we will discuss the dependence of the

optimal clustering coefficient Γ_p^* on the stiffness α.

First we investigate the clustering time t^* of the system as a function of the stiffness α for fixed stability β and density ρ_0. According to Eq. (1), the smaller the stiffness α is, the longer the needed time for the medium reaching the maximum deformation is, and the longer the clustering time of the system is. From the discussion above, one can know that the optimal clustering behavior of the system occurs in the case where the thermal fluctuation approximately balances the effect of the deformation on the motions of particles. Therefore, in the case of optimal clustering one can estimate the optimal clustering stability β_p by the following expression [18]:

$$\beta_p \varepsilon_p^* \approx A, \tag{6a}$$

where ε_p^* is the effective deformation shared by the clustered particles and A is a constant of order $O(1)$. From Fig. 3 we know that the optimal clustering stability β_p is approximately independent of the stiffness α. According to Eq. (6a), the effective deformation ε_p^* is approximately a constant. Employing the relation $\varepsilon_p^* = 1 - e^{-\alpha t_p^*}$, we can obtain that $\alpha t_p^* = \text{const}$. Thus, we have

$$t_p^* \propto \alpha^{-1}. \tag{6b}$$

In Fig. 4(a) we plot the clustering coefficient $\Gamma(t)$ as a function of time t for several different α values at parameters $\beta_p \simeq 5.62$ and $\rho_0 = 0.05$. It can be seen from Fig. 4(a) that the smaller the stiffness α is, the larger the clustering time t_p^* is, and the higher the clustering degree of systems is. These behaviors are consistent with the discussions above. From Fig. 4(a), we can estimate the characteristic time t_p^* corresponding to the characteristic clustering coefficient Γ^*. Figure 4(b) shows the optimal clustering time t_p^* as a function of the stiffness α in log-log scale. It can be seen from Fig. 4(b) that the simulation results are in good agreement with Eq. (6b).

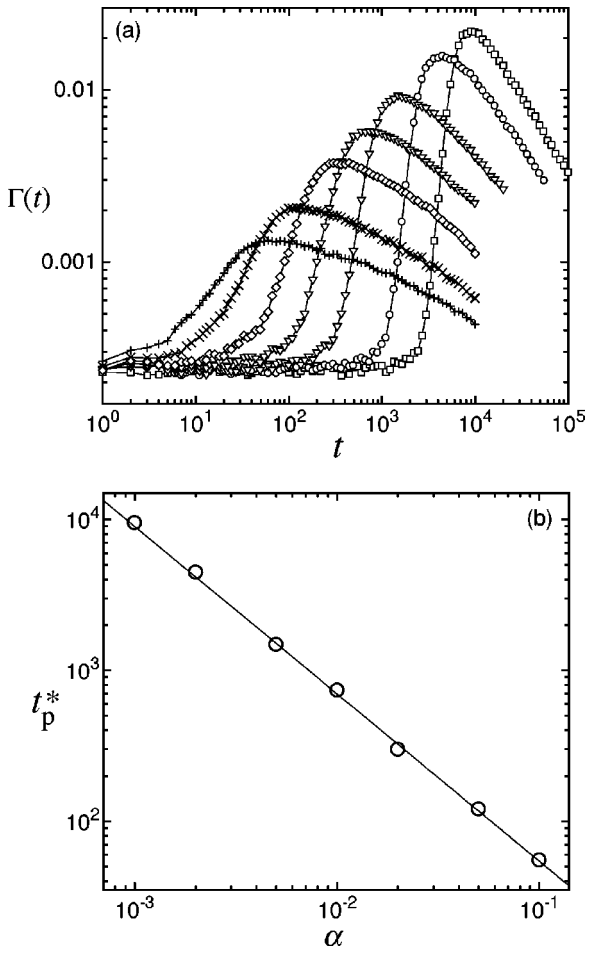

FIG. 4. (a) The evolution of the clustering coefficient $\Gamma(t)$ with time t at the parameters $\beta = 5.62 (\simeq \beta_p)$ and $\rho_0 = 0.05$; from right to left, stiffness $\alpha = 0.001$, 0.002, 0.005, 0.01, 0.02, 0.05, 0.1. (b) The optimal clustering time t_p^* as a function of the stiffness α; the symbols are the simulation results and the line is the fitting plot of Eq. (6b).

Going a step further, we investigate the surface morphology of the deformable medium generated by particles. In the walk, because the motions of particles deform the medium, the surface of the medium becomes rougher and rougher with the passage of time. In the simulations, the roughness of the surface is characterized by the surface width $w(t)$, which is defined by the rms fluctuation in the deformation,

$$w(L,t) \equiv \left(\frac{1}{L^2} \sum_{i=1}^{L} \sum_{j=1}^{L} [\varepsilon(i,j,t) - \overline{\varepsilon}(t)]^2 \right)^{1/2}, \tag{7}$$

where $\overline{\varepsilon}(t)$ is the average deformation per site at the time t. To monitor the roughening process quantitatively we measure the width of the surface as a function of time. Figure 5(a) shows the time evolution of the surface width $w(t)$ for several β values at the stiffness $\alpha = 0.001$ and density $\rho_0 = 0.05$. It can be seen from Fig. 5(a) that the surface width $w(t)$ first increases until a maximum, and then decreases. The behavior in Fig. 5(a) is easy to understand. Initially each site in the medium does not deform and the surface width $w(t)$ is zero. After some time, the motions of particles will deform the medium and the interface becomes rougher and rougher, which leads to an increase in the surface width $w(t)$. When some sites in the lattice reach the maximum deformation, these sites will no longer contribute to the increase of $w(t)$ and the surface width $w(t)$ reaches a maximum. After that the number of sites with a maximum deformation becomes more and more, and the surface width $w(t)$ gradually reduces until the limit value of 0.0 at which all sites in the surface have reached the maximum deformation.

To further understand the roughening process, in Fig. 5(b) we also plot the surface width $w(t)$ as a function of time t in log-log scale. As one can see, there exists a crossover time t_x during the time evolution of the surface width. Initially the surface width $w(t)$ increases as a power of time,

$$w(t) = w_0 t^{\delta}, \quad t \ll t_x, \tag{8}$$

where w_0 is the surface width of the medium at the initial time. The exponent δ, which is called as the growth exponent, characterizes the time-dependent dynamics of the

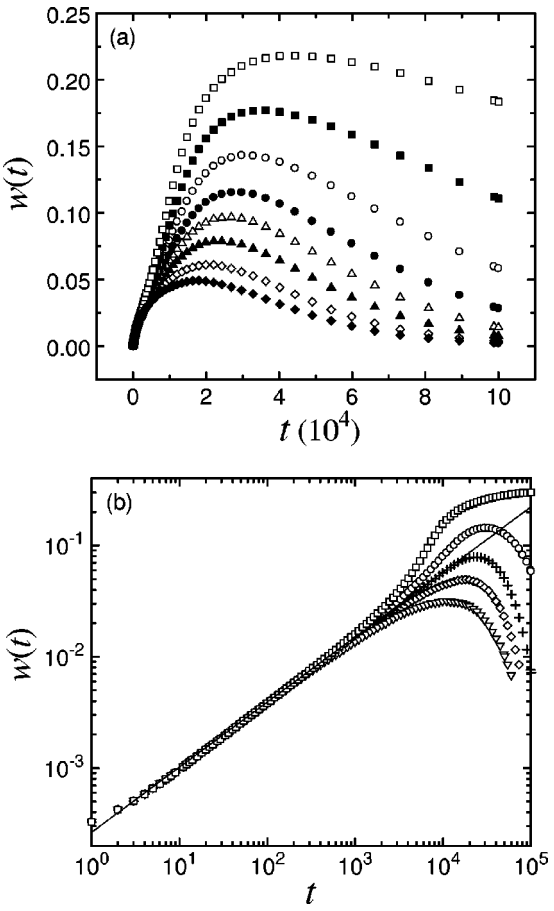

FIG. 5. (a) The evolution of the surface width $w(t)$ of medium with time t at the parameters $\alpha=0.001$ and $\rho_0=0.05$; from bottom to top, stability $\beta=1.12$, 1.41, 1.77, 2.0, 2.24, 2.51, 2.82, 3.16. (b) The log-log plot of the surface width $w(t)$ with the same conditions as (a); from bottom to top $\beta=0.1$, 1.41, 1.77, 2.51, 3.16; the line has a slope of 0.585.

roughening process. From Fig. 5(b), we obtain the growth exponent $\delta\simeq 0.585$. It can also be seen from Fig. 5(b) that there exists a critical roughening stability $\beta_c\approx 1.77$ at which the surface width $w(t)$ shows the best power-law relation and the crossover time t_x has the maximum value. As $\beta<\beta_c$, the curves of the surface width $w(t)$ bend downward, and as $\beta>\beta_c$ the curves bend upward. The existence of the critical stability β_c also results from the competition between the effect of the thermal fluctuation and that of the randomness on the motions of particles [18]. The present critical stability β_c corresponds to the case where the particles begin to cluster, and the optimal stability β_p corresponds the case where the system is the most favorable for the clustering of particles. Therefore, the value of β_c is less than that of β_p, as expected. In addition, we also investigate the cases for the stiffness $\alpha=0.005$, 0.01, and 0.1, respectively. The surface width $w(t)$ shows the similar behavior except the difference of w_0, and the same growth exponent $\delta\simeq 0.585$ is obtained as the case of $\alpha=0.001$.

From the discussions above, we can know that accompanying the clustering of particles, the surface of medium becomes rough and forms a complex landscape with valleys and apexes. The higher the clustering degree of particles is, the rougher the surface of the medium is. Therefore, one can expect that there exists a certain relationship between the clustering degree and the roughness of the surface. To find this relation, for simplicity we assume that the optimal clustering coefficient is directly proportional to the reduced surface width of the medium. Thus, we have

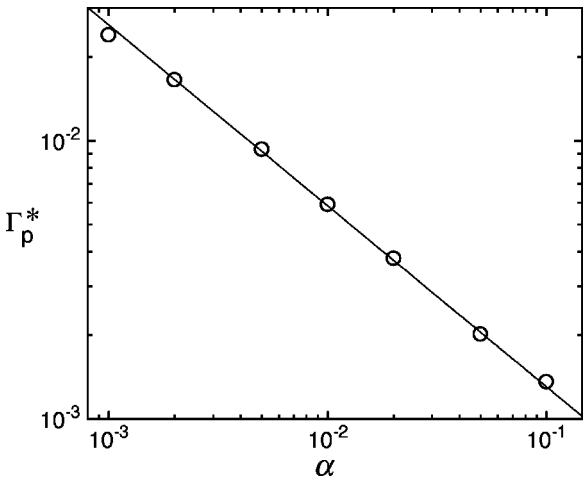

FIG. 6. The optimal clustering coefficient Γ_p^* as a function of the stiffness α at density $\rho_0=0.05$. The symbols are the simulation results and the line is the fitting plot of Eq. (11).

$$\Gamma_p^* \propto \tilde{w}_p^* . \tag{9}$$

The reduced surface width $\tilde{w}(t)=w(t)/w_0$ is independent of the stiffness α for short times. Combining Eqs. (6b) and (8) we obtain

$$\tilde{w}_p^* \propto \alpha^{-\delta}. \tag{10}$$

Comparing Eq. (9) with Eq. (10) and substituting the value of δ, we get

$$\Gamma_p^* \propto \alpha^{-0.585}. \tag{11}$$

Figure 6 plots the optimal clustering coefficient Γ_p^* as a function of the stiffness α in log-log scale. It can be seen from Fig. 6 that the simulation results are in good agreement with Eq. (11). The excellent data consistence supports the proportional assumption in Eq. (9).

We also investigate the dependence of the particle distribution on the average particle density ρ_0. In the investigations, the stiffness of medium is fixed at $\alpha=0.01$, and the particle density ρ_0 takes value ranging from 0.001 to 0.1. The results have shown that the systems have the similar clustering behaviors for different particle densities. Figure 7 plots the characteristic clustering coefficient Γ^* as a function of the stability β for several ρ_0 values at the stiffness $\alpha=0.01$. It can be seen from Fig. 7 that the optimal clustering stability β_p is independent of the particle density ρ_0. However, with the particle density ρ_0 rising, the clustering degree of particles increases drastically.

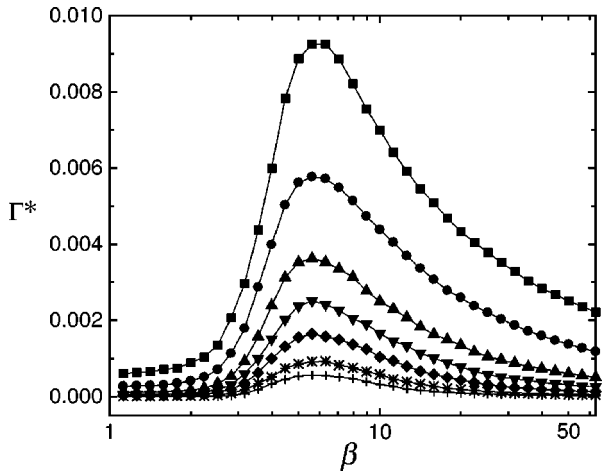

FIG. 7. The characteristic clustering coefficient Γ^* as a function of the stability β at stiffness $\alpha=0.01$; from bottom to top, density $\rho_0=0.001$, 0.002, 0.005, 0.01, 0.02, 0.05, 0.1.

Figure 7 can be understood as follows. When the particle density ρ_0 of systems is larger, the average distance between particles is smaller and the particles have more chances to meet and cluster. Therefore, the clustering degree of particles increases distinctly with the particle density ρ_0 rise. However, the optimal clustering stability β_p is determined by striking a balance between the thermal fluctuation and deformation of the medium, so β_p is not related to ρ_0. As mentioned above, the average particle distance of the system $\overline{d}$ affects the clustering degree of particles. As the average distance $\overline{d}$ decreases, more particles share the same deformation region, and the clustering ability of the system enhances. Since the optimal clustering coefficient Γ_p^* characterizes the clustering degree and clustering ability for the system with a certain α, one can expect that Γ_p^* is inversely proportional to the average distance $\overline{d}$ between particles as

$$\Gamma_p^* \propto 1/\overline{d}. \tag{12a}$$

Employing the relation $\overline{d} \propto (1/\rho_0)^{1/2}$, we obtain

$$\Gamma_p^* \propto \rho_0^{1/2}. \tag{12b}$$

Figure 8 shows the optimal clustering coefficient Γ_p^* as a function of the average particle density ρ_0 in log-log scale. It can be seen from Fig. 8 that the simulation results are in agreement with Eq. (12b). The slight difference between the simulation results and Eq. (12b) may be because of the nonlinear effects of systems.

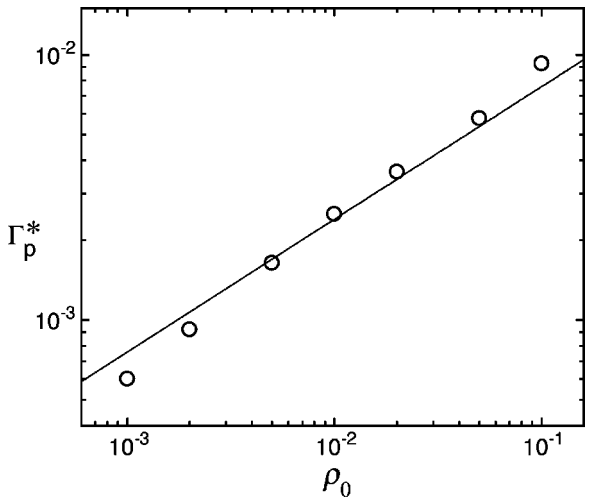

FIG. 8. The optimal clustering coefficient Γ_p^* as a function of the particle density ρ_0 at stiffness $\alpha=0.01$. The symbols are the simulation results and the line is the fitting plot of Eq. (12b).

IV. CONCLUSIONS

We have investigated the multiparticle random walks on a (2+1)-dimensional deformable medium. The evolution of the particle distribution with time is studied. The results show that for the particle distribution there exists a clustering phenomenon in the intermediate time of the evolution. The dependence of the particle distribution on the stiffness of medium α, stability of systems β, and average particle density ρ_0 is also investigated. It shows that at an optimal clustering stability β_p, the system has the highest clustering extent corresponding to a maximum clustering coefficient Γ_p^* for the fixed stiffness α and particle density ρ_0. The optimal clustering stability β_p is almost independent of the stiffness α and density ρ_0. With the increase of the stiffness α, the optimal clustering coefficient Γ_p^* decreases following the relation of $\Gamma_p^* \propto \alpha^{-0.585}$. The relationship between Γ_p^* and ρ_0 can be expressed by $\Gamma_p^* \propto \rho_0^{1/2}$. The surface morphology of the medium is also investigated. It shows that initially the surface width $w(t)$ increases as a power of time with the growth exponent of about 0.585.

ACKNOWLEDGMENT

This work was supported by the National Natural Science Foundation of China.

[1] E.W. Montroll and M.F. Shesinger, in *Nonequilibrium Phenomena II: From Stochastics to Hydrodynamics*, edited by E.W. Montroll and J.L. Lebowitz (North-Holland, Amsterdam, 1984).

[2] B.H. Hughes, *Random Walks and Random Environments* (Clarendon, Oxford, 1995), Vol. 1; G.H. Weiss, *Aspects and Applications of the Random Walk* (North-Holland, Amsterdam, 1994).

[3] F. Wang and D.P. Landau, Phys. Rev. Lett. **86**, 2050 (2001); M. Plapp and A. Karma, *ibid.* **84**, 1740 (2000).

[4] S.-Y. Huang, X.-W. Zou, and Z.-Z. Jin, Phys. Rev. E **65**, 052105 (2002).

[5] J.J. Collins and C.J. De Luca, Phys. Rev. Lett. **73**, 764 (1994); T. Ohira and R. Sawatari, Phys. Rev. E **55**, R2077 (1997).
[6] A. Berrones and H. Larralde, Phys. Rev. E **63**, 031109 (2001); C. Moore and M.E.J. Newman, *ibid.* **61**, 5678 (2000).
[7] A. Ordemann, G. Berkolaiko, S. Havlin, and A. Bunde, Phys. Rev. E **61**, R1005 (2000); A. Ordemann, M. Porto, H.E. Roman, and S. Havlin, *ibid.* **63**, 020104(R) (2001).
[8] P.G. de Gennes, *Scaling Concepts of Polymer Physics* (Cornell University, Ithaca, NY, 1979), and references therein.
[9] D.J. Amit, G. Parisi, and L. Peliti, Phys. Rev. B **27**, 1635 (1983).
[10] C. Domb and G.S. Joyce, J. Phys. C **5**, 956 (1972).
[11] H.E. Stanley, K. Kang, S. Redner, and R.L. Blumberg, Phys. Rev. Lett. **51**, 1223 (1983).
[12] V.B. Sapozhnikov, J. Phys. A **27**, L151 (1994); **31**, 3935 (1998).
[13] A. Ordemann, G. Berkolaiko, S. Havlin, and A. Bunde, Phys. Rev. E **61**, R1005 (2000).
[14] K. Barat and B.K. Chakrabarti, Phys. Rep. **258**, 377 (1995).
[15] Z.-J. Tan, X.-W. Zou, W. Zhang, and Z.-Z. Jin, Phys. Lett. A **289**, 251 (2001).
[16] R.D. Freimuth and L. Lam, in *Modeling Complex Phenomena*, edited by L. Lam and V. Naroditsky (Springer, New York, 1992).
[17] Z.-J. Tan, X.-W. Zou, S.-Y. Huang, W. Zhang, and Z.-Z. Jin, Phys. Rev. E **65**, 041101 (2002).
[18] S.-Y. Huang, X.-W. Zou, W.-B. Zhang, and Z.-Z. Jin, Phys. Rev. Lett. **88**, 056102 (2002).
[19] M.J.B. Krieger, J.-B. Billeter, and L. Keller, Nature (London) **406**, 992 (2000).
[20] S. Hergarten and H.J. Neugebauer, Phys. Rev. Lett. **86**, 2689 (2001).
[21] B. Holldobler and E.O. Wilson, *The Ants* (Springer, Berlin, 1990); E. Bonabeau and G. Theraulaz, Sci. Am. **282**(3), 73 (2000).
[22] J.K. Parrish and L. Edelstein-Keshet, Science **284**, 99 (2000); R.K. Cowen, K.M.M. Lwiza, S. Sponaugle, C.B. Paris, and D.B. Olson, *ibid.* **287**, 857 (2000).
[23] M.F. Shlesinger, Nature (London) **355**, 396 (1992); S.B. Yuste and L. Acedo, Phys. Rev. E **60**, R3459 (1999).
[24] H. Larralde, P. Trunfio, S. Havlin, H.E. Stanley, and G.H. Weiss, Nature (London) **355**, 423 (1992); M. Boguñá, A.M. Berezhkovskii, and G.H. Weiss, Phys. Rev. E **62**, 3250 (2000).
[25] A. Czirók, A.-L. Barabási, and T. Vicsek, Phys. Rev. Lett. **82**, 209 (1999).
[26] T. Vicsek, A. Czirók, E. Ben-Jacob, I. Cohen, and O. Shocher, Phys. Rev. Lett. **75**, 1226 (1995); A. Czirók and T. Vicsek, Physica A **281**, 17 (2000).
[27] N. Shimoyama, K. Sugawara, T. Mizuguchi, Y. Hayakawa, and M. Sano, Phys. Rev. Lett. **76**, 3870 (1996).
[28] H.J. Bussemaker, A. Deutsch, and E. Geigant, Phys. Rev. Lett. **78**, 5018 (1997).
[29] H. Levine, W.-J. Rappel, and I. Cohen, Phys. Rev. E **63**, 017101 (2000).
[30] Z.-J. Tan, X.-W. Zou, S.-Y. Huang, W. Zhang, and Z.-Z. Jin, Phys. Rev. E **66**, 011101 (2002).
[31] S.S. Vyalov, *Rheological Fundamentals of Soil Mechanics* (Elsevier, Amsterdam, 1986); R.M. Christensen, *Theory of Viscoelasticity* (Academic, New York, 1982).
[32] W.-B. Zhang, X.-W. Zou, Z.-Z. Jin, and D.-C. Tian, Physica A **272**, 12 (1999).
[33] T. Vicsek, *Fractal Growth Phenomena* (Singapore, World Scientific, 1992).